Huete, César; Sánchez, Antonio L.; Williams, Forman A. (2014). Linear theory for the interaction of small-scale turbulence with overdriven detonations. *Physics of Fluids*, 26(11), 116101.

DOI: https://doi.org/10.1063/1.4901190

Linear Theory for the Interaction of Small-Scale Turbulence with Overdriven Detonations

César Huete,[1, a)] Antonio L. Sánchez,[1] and Forman A. Williams[1]

Department of Mechanical and Aerospace Engineering,
University of California San Diego, La Jolla, California 92093-0411,
USA

(Dated: Wednesday 22nd October, 2014 10:48)

To complement our previous analysis of interactions of large-scale turbulence with strong detonations, the corresponding theory of interactions of small-scale turbulence is presented here. Focusing most directly on the results of greatest interest, the ultimate long-time effects of high-frequency vortical and entropic disturbances on the burnt-gas flow, a normal-mode analysis is selected here, rather than the Laplace-transform approach. The interaction of the planar detonation with a monochromatic pattern of perturbations is addressed first, and then a Fourier superposition for two-dimensional and three-dimensional isotropic turbulent fields is employed to provide integral formulae for the amplification of the kinetic energy, enstrophy, and density fluctuations. Effects of the propagation Mach number and of the chemical heat release and the chemical reaction rate are identified, as well as the similarities and differences from the previous result for the thin-detonation (fast-reaction) limit.

[a)] Electronic mail: chuete@ucsd.edu

I. INTRODUCTION

In previous work[1] we analyzed the interaction of a strong detonation with inhomogeneous density fields. The motivation was to improve the descriptions of the influence of compressible turbulence on detonation propagation and, in particular, to determine how passage of a planar detonation modifies the turbulence. In that respect, the work complemented the analyses of Jackson *et al.*[2,3], who addressed interactions of detonations with constant-density vorticity fields. It is well known[4] that, excluding acoustic perturbations, which propagate with respect to the fluid, inhomogeneities that travel with the fluid can be decomposed into vortical and entropic components. The earlier work[2,3] had explored the influences of the vortical component, but at high Mach numbers those influences are dominated by influences of the entropic component[5], which therefore was in need of study. The previous investigation[1] provided the additional information that was needed for strong detonations that could be treated as discontinuities.

General reasons for interest in interactions between detonations and turbulence have been discussed and referenced earlier[1], and, since the present paper relies on knowledge of the previous paper, those reasons will not be repeated here. One motivation is improvement in the performance of detonative propulsion devices for hypersonic aircraft, where limited times for fuel-air mixing can pose problems that could be attacked through shock-wave-enhanced mixing[6,7]. In such situations, detonation thicknesses may be larger than the most important representative turbulence scales. The earlier analysis[1] then become inaccurate, and turbulence effects on the evolution of the finite-rate heat release in the interior of the detonation become relevant. The present investigation offers a step towards removing this deficiency.

It is worth observing that numerical studies by Massa *et al.*[8,9] have shown enhanced interactions between turbulence and detonations associated with there being comparable sizes of the inhomogeneities and the unperturbed reaction zones. This increases the interest in pursuing analytical investigations in which turbulence scales are not large compared with reaction-zone thicknesses, for example for testing scaling hypotheses and to determine whether effects of systematic variations of parameters can be derived. Such investigations become quite difficult when the reaction zones and inhomogeneities are of comparable size, but they can be performed accurately when the dimensions of all dis-

turbances are small compared with reaction-zone thicknesses. This is the limit to be addressed here. Inferences concerning behavior at intermediate scales may be derived from resulting functional dependences and comparisons with previous thin-detonation results. Since neither vortical nor entropic fluctuations have yet been considered in this limit, both will be analyzed in the present work.

II. THE STEADY, PLANAR DETONATION

The analysis is a perturbation of the steady, planar ZND detonation structure, a shock followed by an inviscid reaction zone[10–12], for an ideal gas with a constant specific heat at constant pressure. The formulation will be entirely in terms of nondimensional variables. For simplicity, we assume that the rate of energy release per unit volume behind the lead shock $\dot{\bar{q}}$ is uniformly distributed over the thickness of the reaction region, which ends once the fuel is depleted at a finite distance from the shock. This thickness ($\bar{l}$) is taken as the unit of length in the analysis, and the sound velocity $\bar{a}_{\rm N}$ at the Neumann state (just behind of the shock) is taken as the unit of velocity, overbars identifying dimensional quantities. All velocities, both streamwise $\bar{u}$ and transverse $\bar{v}$, as well as sound speeds $\bar{a}$ are nondimensionalized with respect to this same sound velocity, and the conditions at the Neumann state (identified by the subscript N) are also used to normalize the other variables, so that the density $\bar{\rho}$ is normalized by $\bar{\rho}_{\rm N}$, the pressure $\bar{p}$ with $\bar{\rho}_{\rm N}\bar{a}_{\rm N}^2$, and the temperature T by $\bar{T}_{\rm N}$. The subscripts o and b will identify conditions in the fresh mixture and in the burnt gas behind the detonation, respectively, and subscripts l and s will distinguish quantities in the laboratory reference frame in which the fresh mixture is at rest and in the frame moving with the unperturbed detonation, respectively. The three nondimensional parameters that appear in the problem are then the propagation Mach number $M_o = \bar{D}/\bar{a}_o$ of the undisturbed detonation, where $\bar{D}$ is the propagation velocity, the (constant) ratio of specific heats γ, and the total energy released per unit mass of the mixture multiplied by $(\gamma^2-1)/(2\bar{a}_o^2)$, denoted by q. That is, $q = \bar{q}(\gamma^2-1)/(2\bar{a}_o^2)$, where $\bar{q}$ is the heat released per unit mass of mixture, which is related to the heat-release rate by $\dot{\bar{q}} = \bar{\rho}_{\rm N}\bar{u}_{\rm N}\bar{q}/\bar{l}$, with $\bar{u}_{\rm N}$ representing the Neumann streamwise velocity relative to the shock. The nondimensional streamwise and transverse coordinates are x and y, respectively.

Figure 1, in which D denotes the nondimensional propagation velocity of the detona-

tion, illustrates the particle paths and velocity profiles in the laboratory frame of reference. The upstream conditions can be expressed in units of their corresponding Neumann values

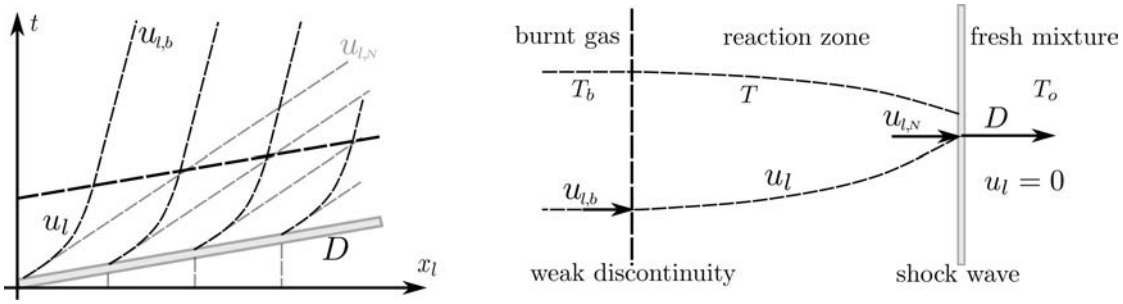

FIG. 1. Schematic fluid particle paths in the laboratory reference frame.

by means of the Rankine-Hugoniot equations, which lead to

$$\rho_o = \frac{\bar{\rho}_o}{\bar{\rho}_{\rm N}} = \frac{(\gamma-1)M_o^2+2}{(\gamma+1)M_o^2} \ , \qquad a_o = \frac{\bar{a}_o}{\bar{a}_{\rm N}} = \frac{(\gamma+1)M_o}{\sqrt{(2\gamma M_o^2-\gamma+1)[(\gamma-1)M_o^2+2]}} \ . \tag{1}$$

The Neumann Mach number, defined as the nondimensional velocity at which the particles leave the shock front is

$$M_{\rm N} = \sqrt{\frac{(\gamma-1)M_o^2+2}{2\gamma M_o^2-\gamma+1}} \ . \tag{2}$$

For strong detonations, M_o is appreciably greater than its Chapman-Jouget value,

$$M_{cj} = \frac{\bar{D}_{cj}}{\bar{a}_o} = \sqrt{1+q}+\sqrt{q} \ , \tag{3}$$

where $\bar{D}_{cj}$ is the Chapman-Jouget detonation propagation velocity. Behind the shock front, the combustion process takes place, and the thermodynamic quantities vary in accordance with the type of heat-deposition involved. To calculate the steady-state profiles of the thermodynamic quantities, it is convenient to write the conservation equations in the shock-fixed reference frame $x_s = Dt - x_l$, where the fluid particles travel with velocity $u_s = D - u_l$. Here $t = \bar{t}\ \bar{l}/\bar{a}_{\rm N}$. After some straightforward algebra, for a constant heat-release rate, the undisturbed pressure profile as a function of the distance from the shock $x_s = [0,1]$ is found to be

$$p = \frac{1+\gamma M_{\rm N}^2}{\gamma(\gamma+1)} + \frac{1}{\gamma+1}\sqrt{(1-M_{\rm N}^2)^2 - (2M_{\rm N}a_o)^2\, q\ x_s} \ , \tag{4}$$

which is related to the velocity profile according to $p = \gamma^{-1} + M_{\rm N}^2 - u_s M_{\rm N}$ and to the density profile, since $\rho = M_{\rm N}/u_s$. The temperature profile is obtained directly from the

perfect-gas equation $T = \gamma p/\rho$, and the dimensionless local speed of sound is then given by $a^2 = T$. At the end of the reaction zone ($x_s = 1$) there is a weak discontinuity that separates the burning and the burnt flow regions; beyond this point, the unperturbed fluid properties remain constant.

III. FORMULATION OF THE PERTURBATION PROBLEM

Complex notation is employed in the normal-mode analysis, with the physical values represented by the real parts. The upstream vortical velocity field is defined in terms of the nondimensional longitudinal u'_o and transverse v'_o perturbations in the laboratory frame of reference as

$$u'_o(x_l, y) = \epsilon_r a_o e^{i(k_x x_l + k_y y)} \ , \qquad v'_o(x_l, y) = -\frac{k_x}{k_y}\epsilon_r a_o e^{i(k_x x_l + k_y y)} \tag{5}$$

where the divergence-free condition $k_x u'_o = -k_y v'_o$ has been applied. The factor ϵ_r represents the amplitude of the upstream velocity disturbances, and it is assumed to be much smaller than unity to remain within the limits of linear theory. Here the wave-number vector $\vec{k}$, with x and y components k_x and k_y, is scaled with the inverse of the detonation thickness $1/\bar{l}$, in accord with our nondimensionalization, so that, in the present analysis, k_x and k_y are large parameters of expansion. Similarly, the density perturbation field is

$$\rho'_o(x_l, y) = \epsilon_e \rho_o e^{i(k_x x_l + k_y y)} \tag{6}$$

where ϵ_e is the nondimensional amplitude, assumed to be small, like ϵ_r. Since the linear responses are independent, no phase angle is imposed between the rotational (subscript r) and entropic (subscript e) perturbations.

Incoming waves from behind the detonation are excluded. When the lead shock encounters the perturbations in (5) and (6), it develops a time-dependent response proportional to $e^{i\omega_s t}$, where the nondimensional frequency is defined as $\omega_s = M_{\rm N} k_x/\rho_o$. The linearized Rankine-Hugoniot relationships then yield for the coefficients of the factor $e^{i(\omega_s t + k_y y)}$ in the nondimensional perturbations

$$i\frac{\omega_s}{k_y}\xi_s = \frac{\gamma+1}{4M_{\rm N}}p'_s + \frac{2\epsilon_r - M_o\epsilon_e}{2}a_o \ , \tag{7a}$$

$$u'_s = \frac{M_o^2+1}{2M_o^2 M_{\rm N}}p'_s + \frac{2\epsilon_r - M_o(1-\rho_o)\epsilon_e}{2}a_o \ , \tag{7b}$$

$$\rho_s' = \frac{1}{M_o^2 M_{\mathrm{N}}^2} p_s' + \epsilon_e \ , \tag{7c}$$

$$v_s' = -iM_{\mathrm{N}} \frac{1-\rho_o}{\rho_o} \xi_s - \frac{\omega_s}{k_y} \frac{a_o \rho_o}{M_{\mathrm{N}}} \epsilon_r \ , \tag{7d}$$

where $\xi_s = k_y \left[x_{l,s}(t) - Dt \right]$ is the amplitude of the perturbation of the shock position. An equation will be derived for p_s' which determines pressure perturbations just behind the shock.

For a given harmonic excitation, such as that considered in (5) and (6), the linear disturbances following the shock front also must be harmonic. At leading order, the perturbations are adiabatic so an acoustic wave form describes the post-shock perturbation field, the acoustic frequency and wave number being related to the shock frequency by the expression $\omega_a = \omega_s - M_{\mathrm{N}} k_{a,\mathrm{N}}$. Evaluating the linear reactive Euler equations at the shock front then yields

$$i\omega_s \rho' + ik_{a,\mathrm{N}} u' + ik_y v' = -\frac{\dot{q}}{1-M_{\mathrm{N}}^2} \left(u' + M_{\mathrm{N}} \rho' \right) \ , \tag{8a}$$

$$i\omega_s u' + ik_{a,\mathrm{N}} p' = -\frac{\dot{q} M_{\mathrm{N}}}{1-M_{\mathrm{N}}^2} \left(u' - M_{\mathrm{N}} \rho' \right) \ , \tag{8b}$$

$$i\omega_s v' + ik_y p' = 0 \ , \tag{8c}$$

$$i\omega_s p' - i\omega_s \rho' = \frac{\dot{q}}{1-M_{\mathrm{N}}^2} \left[\left(1-M_{\mathrm{N}}^2\right) u' + M_{\mathrm{N}} \rho' - \gamma M_{\mathrm{N}} p' \right] \ , \tag{8d}$$

where the dimensionless acoustic wavenumbers $k_{a,\mathrm{N}}$ and k_y come from the streamwise and lateral derivatives, respectively, and the dimensionless frequency ω_s is obtained from the material derivative following the shock front. At leading order, $\dot{q} = 0$, the well-known adiabatic dispersion relationship is recovered, $\omega_{a,\mathrm{N}}^2 = k_{a,\mathrm{N}}^2 + k_y^2$. The dimensionless acoustic wavenumber $k_{a,\mathrm{N}}$ and the associated frequency are

$$k_{a,\mathrm{N}} = \frac{M_{\mathrm{N}} \omega_s - \sqrt{\omega_s^2 - \left(1-M_{\mathrm{N}}^2\right) k_y^2}}{1-M_{\mathrm{N}}^2} \ , \qquad \omega_{a,\mathrm{N}} = \frac{\omega_s - M_{\mathrm{N}} \sqrt{\omega_s^2 - \left(1-M_{\mathrm{N}}^2\right) k_y^2}}{1-M_{\mathrm{N}}^2} \ . \tag{9}$$

The effect of the chemical reaction enters through the dimensionless rate of heat release

$$\dot{q} = \frac{2a_o^2 q}{\gamma+1} = \frac{\dot{\bar{q}} \bar{l} (\gamma-1)}{\bar{\rho}_{\mathrm{N}} \bar{u}_{\mathrm{N}} \bar{a}_{\mathrm{N}}^2} \ , \tag{10}$$

which is scaled with use made of the detonation thickness $\bar{l}$ and the unperturbed enthalpy flux at the Neumann state $\bar{\rho}_{\mathrm{N}} \bar{u}_{\mathrm{N}} \bar{a}_{\mathrm{N}}^2 / (\gamma - 1)$.

There can be stable acoustic radiation right behind the shock wave if $\omega_s > (1 - M_{\rm N})^{1/2} k_y$, but if $\omega_s < (1 - M_{\rm N})^{1/2} k_y$ then these pressure perturbations are evanescent (waves whose amplitudes exponentially decay behind the shock front)[13]. The latter condition corresponds to the square roots in (9) becoming imaginary, contributing exponential rather than oscillatory behavior, which must decay to satisfy the boundary conditions. The shock oscillation frequency is conveniently described in terms of a dimensionless frequency ζ,

$$\zeta = \frac{M_{\rm N}}{\rho_o \sqrt{1 - M_{\rm N}^2}} \frac{k_x}{k_y} = \frac{M_{\rm N}}{\rho_o \sqrt{1 - M_{\rm N}^2}} \frac{1}{\tan\theta} = \frac{1}{\sqrt{1 - M_{\rm N}^2}} \frac{\omega_s}{k_y} \ , \tag{11}$$

θ being the angle between the incident wavenumber $\vec{k}$ and the direction of propagation of the unperturbed detonation. It is useful to define ζ in this manner here because acoustic radiation can then occur for $\zeta \geq 1$ but the acoustics is evanescent for $\zeta < 1$. The wavelength of the downstream disturbances are long for $\zeta < 1$ and short $\zeta \geq 1$, and therefore solutions for $\zeta \geq 1$, the high-frequency solutions that appear for small angles θ, are called short-wavelength solutions, while those corresponding to the low-frequency, large-θ range $\zeta < 1$ are called long-wavelength solutions. By introducing an expansion up to terms of order k_y^{-1}, equations (7) and (8) can be combined to yield

$$\underbrace{\frac{-\omega_a^2 a_{20} + \omega_a k_a a_{11} - k_a^2 a_{02} + k_y^2 a_{00}}{k_y^2} p_s'}_{O(\epsilon)} + \underbrace{i \frac{\omega_s}{k_y^2} a_{\rm R} \dot{q} \ p_s'}_{O(\epsilon \ k_y^{-1})} = \underbrace{\frac{(M_{\rm N}^2 k_y^2 - \rho_o \omega_s^2)}{k_y^2} b_2}_{O(\epsilon)} - \underbrace{i \frac{\omega_s}{k_y^2} b_{\rm R} \dot{q}}_{O(\epsilon \ k_y^{-1})} \tag{12}$$

plus terms of order ϵk_y^{-2}, where

$$\begin{aligned}
a_{20} &= \frac{M_o^2 + 1 + 2M_{\rm N}^2 M_o^2}{2M_{\rm N} M_o^2} \ , \qquad a_{11} = \frac{M_o^2(2 + M_{\rm N}^2) + 1}{M_o^2} \ , \qquad a_{02} = \frac{(3M_o^2 + 1)\, M_{\rm N}}{2M_o^2} \ , \\
a_{\rm R} &= \frac{[(M_o^2 + 1)\,(1 + M_{\rm N}^2) - 2\,(1 - \gamma M_o^2 M_{\rm N}^2)]}{2M_o^2\,(1 - M_{\rm N}^2)} \ , \qquad a_{00} = \frac{M_{\rm N}(1 - \rho_o)(\gamma + 1)}{4\rho_o} \ , \\
b_2 &= \frac{a_o(1 - \rho_o)(M_o \epsilon_e - 2\epsilon_r)}{2\rho_o} \ , \qquad b_{\rm R} = \frac{[(a_o - \rho_o a_o - 2) M_{\rm N} \epsilon_e - a_o \epsilon_r]\, M_{\rm N}}{2(1 - M_{\rm N}^2)} \ .
\end{aligned} \tag{13}$$

Equation (12) is the generalization of the well-known expression for the response of the pressure behind the shock wave, accounting for the exothermic finite-rate chemistry in the heat-release zone of the detonation that follows the shock. The present contribution analyzes the influences of the terms involving $a_{\rm R}$ and $b_{\rm R}$ which describe this effect. It is worthwhile to note that these influences depend only on the local effect caused by the rate of heat release $\dot{q}$ right behind the shock. The profile of the heat-release rate

downstream becomes irrelevant. These results thus will be general in the sense that they are independent of the particular model that produced (4). All that is required is that there be no regions of rapid heat-release rate. With the length $\bar{l}$ defined in terms of the average rate of heat release, the parameter k_y^{-1} must be small.

Although the formulation leading to (12) is then independent of the heat-release processes occurring downstream, those processes do affect the disturbances that occur within the thick detonation and downstream therefrom. As is well known from the earlier investigations, those disturbances can be considered to be of two general types, namely acoustic fluctuations that propagate downstream with respect to the fluid locally and fluctuations that remain fixed with respect to the fluid particles. In the present notation, the former are proportional to $e^{i(\omega_s t + k_a x_s + k_y y)}$, and the latter are proportional to $e^{i[\omega_s t - (\rho/\rho_o) k_x x_s + k_y y]}$. Here

$$k_a = \frac{M\omega_s - \sqrt{\omega_s^2 - a^2\left(1-M^2\right)k_y^2}}{a\left(1-M^2\right)} \tag{14}$$

for the acoustic component, and the corresponding acoustic frequency experienced by a fluid element moving with the local fluid speed is

$$\omega_a = \frac{\omega_s - M\sqrt{\omega_s^2 - a^2\left(1-M^2\right)k_y^2}}{1-M^2} \ . \tag{15}$$

The results to be given below pertain to the coefficients of these disturbances, in particular as the fluctuations emerge into the burnt gas. There are contributions to theses modification associated with passage through the heat-release region at order ϵ as well as order ϵk_y^{-1}. The former, however, turn out to be of the same functional form in the burnt gas as those derived in previous studies of thin detonations, but with coefficients corresponding instead to passage through the lead shock only. Unlike the thin detonation, the thick detonation does not modify the amplitudes from those of the lead shock. Aside from this difference, the results are identical in the two limits. Attention therefore will be focused on the fluctuations of order ϵk_y^{-1}.

IV. RESULTS OF THE PERTURBATION ANALYSIS

In terms of the expansions in (12), the results are quite different, depending on whether the acoustics is radiating ($\zeta \geq 1$) or evanescent ($\zeta < 1$). For radiating conditions, there is

no contribution at order k_y^{-1}, and so the first correction that involves the heat release q directly is of order k_y^{-2}, beyond the range of the current analysis. The perturbations to be derived here that explicitly involve q therefore are restricted to the evanescent conditions that occur at the larger angles θ that produce $\zeta < 1$. Otherwise the results from (12) are the same as those for nonreacting shocks.

The aforementioned indirect effect of the heat release in the detonations on the acoustic perturbations at leading order do, however, influence the final radiation condition. As a consequence of the variation of the quantities M and a with the distance behind the shock, the condition for the detonation to be radiating at its downstream boundary is $\zeta > \zeta_b$, where

$$\zeta_b = \sqrt{\frac{1 - M_b^2}{1 - M_{\rm N}^2}} a_b \ , \tag{16}$$

which is plotted in Fig. 2 as a function of $f-1$ (where $f = M_o^2/M_{cj}^2$ is the overdrive factor), showing that it can be greater or less than unity. For sufficiently weak overdrive, ζ_b is less than unity, and so, when $\zeta < 1$, radiating conditions are encountered at some point within the detonation, but the exponential decay of the evanescent wave from the shock before that will render the amplitude of the radiated wave negligible small for thick detonations, whence it is not considered here. On the other hand, especially at the higher values of the heat release parameter q, above a critical overdrive ζ_b becomes greater than unity, in which case an evanescent shock will always correspond to an evanescent detonation. The relevant parameter therefore in every case is ζ, and the perturbations calculated here are all for downstream conditions that are effectively evanescent

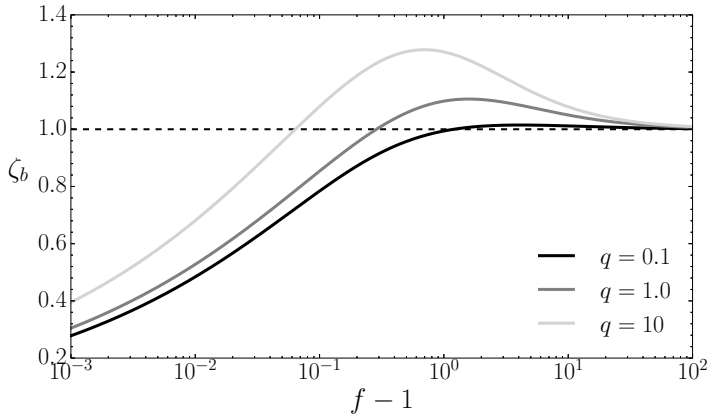

FIG. 2. Frequency ζ_b for $\gamma = 1.2$ as a function of M_o for different heat releases $q = 0.1, 1, 10$.

Because of the dominance of the lead shock for thick detonations, the amplitudes of the perturbation at order ϵ are the same as those derived previously for shock-vorticity interactions ($\epsilon_e = 0$)[13,14] and for shock-density interactions ($\epsilon_r = 0$)[15]. Since there are no perturbations at order ϵk_y^{-1} for radiating acoustics ($\zeta \geq 1$) the exothermicity does not affect the amplitudes of the radiated acoustic fields at this order. The amplitudes of the evanescent fields are, however, affected. To describe such effects, the acoustic pressure fluctuations in the burnt gas at this order can be represented as $\epsilon \dot{q} k_y^{-1} C_p e^{i(\omega_s t + k_{a,b} x_s + k_y y)}$, where $k_{a,b}$, having a positive imaginary part in this case, is given by (14) with $M = M_b$ and $a = a_b$. The factor $\dot{q}$ is included here because these corrections are proportional to $\dot{q}$. Since overall phase angles are irrelevant for subsequent statistical averages, the complex coefficients C_p will not be given here; instead only $A_p = \pm|C_p|$ will be given, with the positive sign selected for contributions that increase the amplitude of the perturbation of order ϵ and the negative sign for perturbations that decrease that amplitude. With this convention, it is found that

$$A_{pr} = \frac{B_{pr}\left[(M_o^2+1)\left(1+M_{\rm N}^2\right) - 2\left(1-\gamma M_o^2 M_{\rm N}^2\right)\right] - a_o M_o^2 M_{\rm N}}{\left[4M_o^4 M_{\rm N}^2\zeta^2(1-\zeta^2) + \left[(M_o^2+1)\zeta^2 - M_o^2\right]^2\right]^{3/2}} \times \\ \times \frac{4M_o^2 M_{\rm N}^2 \zeta^2 \sqrt{1-\zeta^2}\left[(M_o^2+1)\zeta^2 - M_o^2\right]}{(1-M_{\rm N}^2)^{3/2}} \tag{17a}$$

and

$$A_{pe} = -\frac{B_{pe}\left[(M_o^2+1)\left(1+M_{\rm N}^2\right) - 2\left(1-\gamma M_o^2 M_{\rm N}^2\right)\right] + M_o^2 M_{\rm N}^2(a_o - a_o\rho_o - 2)}{\left[4M_o^4 M_{\rm N}^2\zeta^2(1-\zeta^2) + \left[(M_o^2+1)\zeta^2 - M_o^2\right]^2\right]^{3/2}} \times \\ \times \frac{4M_o^2 M_{\rm N}^2 \zeta^2 \sqrt{1-\zeta^2}\left[(M_o^2+1)\zeta^2 - M_o^2\right]}{(1-M_{\rm N}^2)^{3/2}} \ , \tag{17b}$$

where the subscripts r and e identify the rotational and entropic contributions to ϵ, respectively. The factors B_{pr} and B_{pe} refer to the pressure disturbances generated by the inert shock (see appendix for details) and are given by

$$B_{pr} = \frac{2M_o M_{\rm N}^2(1-\rho_o)\left[(M_o^2+1)\zeta^2 - M_o^2\right]\left[M_{\rm N}^2 - \rho_o\left(1-M_{\rm N}^2\right)\zeta^2\right]}{\rho_o^2\left(1-M_{\rm N}^2\right)\left[4M_o^4 M_{\rm N}^2\zeta^2(\zeta^2-1) + \left((M_o^2+1)\zeta^2 - M_o^2\right)^2\right]} \tag{18}$$

and

$$B_{pe} = -\frac{M_o^2 M_{\rm N}^2(1-\rho_o)\left[(M_o^2+1)\zeta^2 - M_o^2\right]\left[M_{\rm N}^2 - \rho_o\left(1-M_{\rm N}^2\right)\zeta^2\right]}{\rho_o^2\left(1-M_{\rm N}^2\right)\left[4M_o^4 M_{\rm N}^2\zeta^2(\zeta^2-1) + \left((M_o^2+1)\zeta^2 - M_o^2\right)^2\right]} \ . \tag{19}$$

In a similar manner, if the contributions to the density and vorticity fluctuations in the burnt gas at order ϵk_y^{-1} are denoted by $\epsilon \dot{q} k_y^{-1} C_\rho e^{i[\omega_s t + \frac{\rho_b}{\rho_o} x_s + k_y y]}$ and $\epsilon \dot{q} k_y^{-1} C_\omega e^{i[\omega_s t + \frac{\rho_b}{\rho_o} x_s + k_y y]}$,

respectively, then results are given for $A_\rho = \pm|C_\rho|$ and $A_\omega = \pm|C_\omega|$, the signs similarly being selected according to the influence on the perturbations of order ϵ. It is then found that

$$A_{\rho r} = \frac{(1 - M_o^2 M_{\rm N}^2)}{M_o^2 M_{\rm N}^2} A_{pr} \ , \tag{20a}$$

$$A_{\rho e} = \frac{(M_o^2 M_{\rm N}^2 - 1)\left[M_o^2 M_{\rm N}^2 + 2\left(1 - M_o^2 M_{\rm N}^2\right) B_{pe}\right]}{2 M_o^4 M_{\rm N}^4 B_{\rho e}} \times \\ \times \frac{\sqrt{4 M_o^4 M_{\rm N}^2 \zeta^2 (1-\zeta^2) + \left[(M_o^2+1)\zeta^2 - M_o^2\right]^2}}{\left[(M_o^2+1)\zeta^2 - M_o^2\right]} A_{pe}, \tag{20b}$$

and, with the Ω's defined in the appendix,

$$A_{\omega r} = \frac{\Omega_2 \left(\Omega_1 + 2\Omega_2 B_{pr}\right) \sqrt{4 M_o^4 M_{\rm N}^2 \zeta^2 (1-\zeta^2) + \left[(M_o^2+1)\zeta^2 - M_o^2\right]^2}}{2\left[(M_o^2+1)\zeta^2 - M_o^2\right] B_{\omega r}} A_{pr} \ , \tag{21a}$$

$$A_{\omega e} = -\frac{\Omega_2 \left(\Omega_3 + 2\Omega_2 B_{pe}\right) \sqrt{4 M_o^4 M_{\rm N}^2 \zeta^2 (1-\zeta^2) + \left[(M_o^2+1)\zeta^2 - M_o^2\right]^2}}{2\left[(M_o^2+1)\zeta^2 - M_o^2\right] B_{\omega e}} A_{pe} \ , \tag{21b}$$

where $B_{\rho e}$, $B_{\omega r}$, and $B_{\omega e}$ are the order ϵ contributions for the long-wavelength entropic and vorticity perturbations (see appendix for details) and are given by

$$B_{\rho e} = \left[\left(\frac{1 - M_o^2 M_{\rm N}^2}{M_o^2 M_{\rm N}^2} B_{pe} + 1\right)^2 + \left(\frac{1 - M_o^2 M_{\rm N}^2}{M_o^2 M_{\rm N}^2} B'_{pe}\right)^2\right]^{1/2} \ , \tag{22}$$

$$B_{\omega r} = \left[\left(\Omega_1 + \Omega_2 B_{pr}\right)^2 + \left(\Omega_2 B'_{pr}\right)^2\right]^{1/2} \ , \quad B_{\omega e} = \left[\left(\Omega_3 + \Omega_2 B_{pe}\right)^2 + \left(\Omega_2 B'_{pe}\right)^2\right]^{1/2} \ . \tag{23}$$

The velocity field is also modified at order ϵk_y^{-1} as a consequence of the associated vorticity perturbations. The corresponding $A_{(u,v)r}$ and $A_{(u,v)e}$ are provided in (A10) and (A12), respectively.

V. PREDICTIONS FOR MONOCHROMATIC DISTURBANCES

In viewing the corrections proportional to $\epsilon \dot{q} k_y^{-1}$ it is helpful to plot the results in Eqs. (20) and (21) for selected values of M_o and γ, because the formulas are too complicated for simple conclusions to be readily drawn directly from them. Since the results vary strongly with θ as the critical orientation is approached, their characteristics are seen most clearly on a log scale of $1 - \zeta$. In Fig. 3 such plots for the coefficients A_ρ and

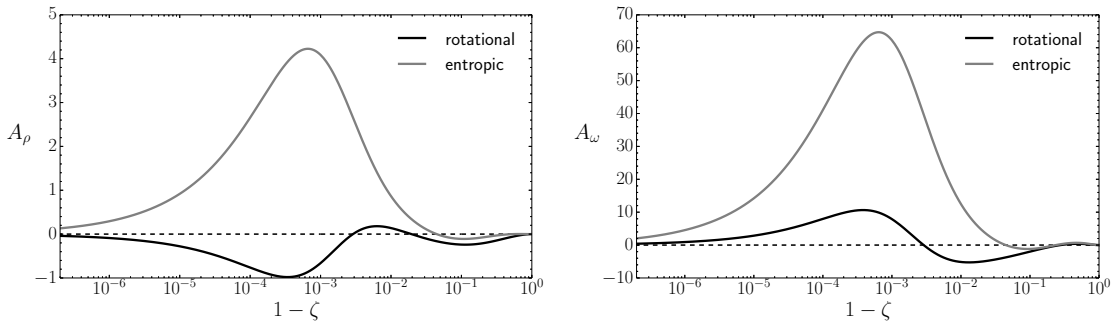

FIG. 3. Exothermic contribution for the density A_ρ and vorticity A_ω fields as a function of $1-\zeta$ for $M_o = 5$ and $\gamma = 1.2$.

A_ω therefore are shown for the representative values $M_o = 5$ and $\gamma = 1.2$. The general characteristics of the results are the same for other values of these parameters.

All the curves have certain attributes in common. For example, all of the corrections approach zero as $1-\zeta$ approaches zero and unity, which, according to (11), correspond, respectively, to the critical angle θ and to the detonation encountering the perturbation field edge-on. It is understandable that an edge-on encounter will not have any effect, and since the corrections are of higher order for the angles of encounter between normal and the critical angle (that is, at the higher frequencies), considerations of continuity suggest that the approach to zero at the critical angle is reasonable. In addition, all of the curves achieve both negative and positive values, although, for purely entropic initial perturbations, the range and extent of the negative segment are very small. The curves, in general, exhibit oscillations, in that they pass through zero once or twice. This complicates the task of drawing general conclusions.

Since the logarithmic scale in Fig. 3 accentuates the range as the critical angle is approached, in determining the dominant overall effect, the scale variation must be considered. With this in mind, it may be inferred from the curves that the corrections are mainly positive for entropic upstream disturbances and mainly negative for rotational upstream disturbances. It was found that the heat release in thin detonations tends to reduce fluctuations for entropic upstream fluctuations[1]. Although the curves in the earlier paper[2] at first glance suggest otherwise, in fact, with the current scaling, the same is true for rotational fluctuations[2]. Hence, the present thick-detonation results are in opposite directions from the thin-detonation results for entropic upstream disturbances but in

the same direction for rotational disturbances. This suggests that entropic disturbances, which tend to be dominant at high Mach numbers, may experience enhanced responses at intermediate sizes.

VI. STATISTICAL AVERAGES FOR INTERACTIONS WITH ISOTROPIC TURBULENCE

Statistical averages for turbulent flows are generated from the preceding results by integrating the square amplitudes of the perturbations over the spectrum of wave numbers. As in previous work[1,3], the upstream flow is assumed to be homogeneous and isotropic so that the wave-number vector $\vec{k}$ is uniformly distributed over the unit sphere (or around the unit semicircle in two dimensions). Therefore, the analyses consists of a superposition of linear perturbations whose amplitudes are functions only of the wave-number amplitude $|\vec{k}|$[16]. Averaged quantities of interest include the kinetic energy K, the enstrophy W, and the density G.

When considering the interaction with a two-dimensional isotropic vorticity field, the velocity field is represented by divergence-free velocity disturbances $\mathbf{v}'_o = \epsilon_k a_o(\sin\theta, \cos\theta)$, whose associated wave-number vector is $\vec{k} = k(-\cos\theta, \sin\theta)$. The mean square of the longitudinal and transverse velocity perturbations are[3,14,17,18]

$$\langle u_o'^2\rangle_{2D} = \langle v_o'^2\rangle_{2D} = \frac{\pi}{2} a_o^2 \int_0^\infty \epsilon_k(k)^2 k \mathrm{d}k \ . \tag{24}$$

Thanks to isotropy upstream, the spectrum contribution $\int_0^\infty \epsilon_k(k)^2 k\mathrm{d}k$ is factored out. It then becomes possible to eliminate this factor in expressing results as ratios of post-detonation intensities to upstream intensities. The three-dimensional problem is conveniently formulated in spherical polar coordinates, so the upstream velocity field is $\mathbf{v}'_o = a_o\epsilon_k(\sin\theta, \cos\theta\cos\varphi, \cos\theta\sin\varphi)$ and the associated wave-number vector is $\vec{k} = k(-\sin\theta, \cos\theta\sin\varphi, \cos\theta\cos\varphi)$. The upstream mean-square disturbances are expressed as [3,14,17,18]

$$\langle u_o'^2\rangle_{3D} = \frac{8\pi}{3} a_o^2 \int_0^\infty \epsilon_k(k)^2 k^2 \mathrm{d}k \ , \quad \langle v_o'^2\rangle_{3D} = \langle w_o'^2\rangle_{3D} = \frac{2\pi}{3} a_o^2 \int_0^\infty \epsilon_k(k)^2 k^2 \mathrm{d}k \tag{25}$$

in that case. If there are only density disturbances ahead of the detonation wave, then

the statistical averages under the same isotropy assumptions are[1,15,19]

$$\langle \rho_o'^2 \rangle_{\rm 2D} = \rho_o^2 \pi \int_0^\infty \epsilon_e(k)^2 k {\rm d}k \ , \qquad \langle \rho_o'^2 \rangle_{\rm 3D} = \rho_o^2 4\pi \int_0^\infty \epsilon_e(k)^2 k^2 {\rm d}k \ , \tag{26}$$

where $\epsilon_e(k)$ represents the normalized internal-energy spectrum. In all cases results are given as ratios of final to initial normalized intensities, independent of the particular spectral distributions.

Consistent with the monochromatic perturbations to the inert lead-shock results being proportional to $\dot{q}k_y^{-1}$ with respect to the order-ϵ base-case perturbations, for isotropic turbulence the corresponding relative perturbations to the statistical averages will be of order $\dot{q}|k|^{-1}$. The interest here therefore focuses on corrections of order $\epsilon\dot{q}|k|^{-1}$ to the order-ϵ base-case predictions of the changes in the statistical averages. With $K_{\rm B}$ denoting the order-unity ratio of the normalized post-detonation turbulent kinetic energy (normalized by the sound speed at the Neumann state) to the normalized upstream turbulent kinetic energy (normalized by the sound speed in the fresh mixture) and $K_{\rm A}$ denoting the order-unity coefficient of the correction to this ratio of order $\dot{q}|k|^{-1}$, interest then rests on the fractional correction $\dot{q}|k|^{-1}\Delta_{\rm K}$, where $\Delta_{\rm K} = K_{\rm A}/K_{\rm B}$ is a quantity of order unity that is independent of $\dot{q}$ and depends only on M_o and γ. While this definition is useful for rotational turbulent fluctuations, it clearly cannot be applied if the upstream fluctuations are purely entropic. In that case, as in earlier work[1], $K_{\rm B}$ is defined as a normalized post-detonation turbulent kinetic energy divided by the mean-square fresh-mixture density fluctuations normalized by the average density of the fresh mixture. However, instead of employing the burnt-gas sound speed for normalizing the post-detonation turbulent kinetic energy, as earlier[1], now the Neumann-state sound speed is used for that purpose, because otherwise and additional dependence on $\dot{q}$ arises. With this revised normalization and $K_{\rm B}$ again denoting the order-unity ratio for the post-detonation turbulent kinetic energy and $K_{\rm A}$ the order-unity coefficient of the correction of order $\dot{q}|k|^{-1}$, the order-unity measure $\Delta_{\rm K} = K_{\rm A}/K_{\rm B}$ is to be exhibited here. The additional subscripts r and e will distinguish whether rotational or entropic fluctuations are considered, as before.

There are similar breakdowns for enstrophy and density. Here, too, to avoid introducing an additional dependence on $\dot{q}$, the post-detonation enstrophy and density fluctuations are normalized by properties at the Neumann state, while the upstream perturbations are normalized , as always, by the upstream mean properties. In this way, the associated order-

unity corrections are $\Delta_{\rm W} = W_{\rm A}/W_{\rm B}$ and $\Delta_{\rm G} = G_{\rm A}/G_{\rm B}$. Even though the initial turbulence is isotropic, the interaction with the shock induces anisotropy, and there may be interest separately in longitudinal velocity fluctuations (velocities in the direction of detonation propagation) and transverse velocity fluctuations (velocities transverse to the propagation direction). The longitudinal and transverse contributions to the kinetic-energy ratio for K are denoted by L and T, respectively, and results for $\Delta_{\rm L} = L_{\rm A}/L_{\rm B}$ and for $\Delta_{\rm T} = T_{\rm A}/T_{\rm B}$ also will be given. Specific definitions appear in the following sub-sections.

A. Turbulent kinetic-energy amplification

For rotational upstream disturbances, following Refs.[3,13,14], amplification factors for turbulent kinetic energy are defined as

$$K = \frac{\langle \bar{\mathbf{v}}_b'^2 \rangle_{\rm 2D}}{\langle \bar{\mathbf{v}}_o'^2 \rangle_{\rm 2D}} = \frac{2}{\pi a_o^2} \int_0^{\pi/2} \left(|u_b'|^2 + |v_b'|^2 \right) \sin^2\theta \mathrm{d}\theta = \frac{1}{2a_o^2} \int_0^{\infty} \left(|u_b'|^2 + |v_b'|^2 \right) \mathcal{P}_r \mathrm{d}\zeta \tag{27a}$$

and

$$K = \frac{\langle \bar{\mathbf{v}}_b'^2 \rangle_{\rm 3D}}{\langle \bar{\mathbf{v}}_o'^2 \rangle_{\rm 3D}} = \frac{1}{2a_o^2} \int_0^{\pi/2} \left(|u_b'|^2 + |v_b'|^2 \right) \sin^3\theta \mathrm{d}\theta + \frac{1}{2} = \frac{1}{3a_o^2} \int_0^{\infty} \left(|u_b'|^2 + |v_b'|^2 \right) \mathcal{P}_r \mathrm{d}\zeta + \frac{1}{2} \ , \tag{27b}$$

for two-dimensional and three-dimensional disturbances, respectively, where the functions $|u_b'|$ and $|v_b'|$ refer to the longitudinal and transverse velocity perturbation amplitudes in the burnt gas, and the normalized probability-density distributions are

$$\mathcal{P}_r(\zeta) = \frac{4}{\pi} \frac{M_{\rm N}^3 \rho_o \sqrt{1 - M_{\rm N}^2}}{\left[M_{\rm N}^2 + \zeta^2 \rho_o^2 \left(1 - M_{\rm N}^2 \right) \right]^2} \ , \quad \mathcal{P}_r(\zeta) = \frac{3}{2} \frac{M_{\rm N}^4 \rho_o \sqrt{1 - M_{\rm N}^2}}{\left[M_{\rm N}^2 + \zeta^2 \rho_o^2 \left(1 - M_{\rm N}^2 \right) \right]^{5/2}} \ , \tag{28}$$

for the two-dimensional and three-dimensional cases, respectively. The factors $M_{\rm N}^2 + \zeta^2 \rho_o^2 \left(1 - M_{\rm N}^2 \right)$, which appear throughout, arise through Eq. (11) in converting integrations over θ to integrations over ζ. The breakdown $K = K_{\rm B} + \dot{q}|k|^{-1} K_{\rm A}$ may also be divided into the longitudinal and transverse components, according to $K = (1/2)(L + T)$ in two dimensions and $K = (1/3)(L+2T)$ in three dimensions. The three-dimensional case can be simplified so as to deal with an equivalent two-dimensional problem by choosing a reference frame that leaves one of the velocity contributions invariant. The base-component terms, which account for the rotational and acoustic contributions at order ϵ, are provided in the appendix in (A13) and (A14) and also in literature[13,14]. The corresponding quantities at

order $\epsilon\dot{q}|k|^{-1}$ are

$$L_{\mathrm{A}r} = \frac{2}{a_o^2}\int_0^1 |B_{ur}|A_{ur}\left[1+\zeta^2\rho_o^2\left(M_{\mathrm{N}}^{-2}-1\right)\right]^{1/2}\mathcal{P}_r\mathrm{d}\zeta \tag{29a}$$

for both two and three dimensions, and

$$T_{\mathrm{A}r} = \frac{2}{a_o^2}\int_0^1 |B_{vr}|A_{vr}\left[1+\zeta^2\rho_o^2\left(M_{\mathrm{N}}^{-2}-1\right)\right]^{1/2}\mathcal{P}_r\mathrm{d}\zeta\ , \tag{29b}$$

$$T_{\mathrm{A}r} = \frac{1}{a_o^2}\int_0^1 |B_{vr}|A_{vr}\left[1+\zeta^2\rho_o^2\left(M_{\mathrm{N}}^{-2}-1\right)\right]^{1/2}\mathcal{P}_r\mathrm{d}\zeta\ , \tag{29c}$$

for two dimensions and three dimensions, respectively. The factor $[1+\zeta^2\rho_o^2\left(M_{\mathrm{N}}^{-2}-1\right)]^{1/2}$, which does not appear for the base-contribution factors, arises from the equality $|k|/k_y = (\sin\theta)^{-1}$. The amplitudes of the base velocity fluctuations B_{ur} and B_{vr} that appear here are provided in (A9a), and the corrections A_{ur} and A_{vr} are given in (A10).

As explained above, when the upstream perturbations are purely entropic the ratio K is normalized as in Ref.[1], which results in

$$K = \frac{\langle\mathbf{v}_b'^2\rangle_{\mathrm{2D}}}{\pi\int_0^\infty \epsilon_e(k)^2 k\mathrm{d}k} = \int_0^\infty \left(|u_b'|^2+|v_b'|^2\right)\mathcal{P}_e\mathrm{d}\zeta \tag{30a}$$

and

$$K = \frac{\langle\mathbf{v}_b'^2\rangle_{\mathrm{3D}}}{4\pi\int_0^\infty \epsilon_e(k)^2 k^2\mathrm{d}k} = \int_0^\infty \left(|u_b'|^2+|v_b'|^2\right)\mathcal{P}_e\mathrm{d}\zeta \tag{30b}$$

for the two-dimensional and three-dimensional cases, where the corresponding normalized probability density functions are

$$\mathcal{P}_e(\zeta) = \frac{2}{\pi}\frac{M_{\mathrm{N}}\rho_o\sqrt{1-M_{\mathrm{N}}^2}}{M_{\mathrm{N}}^2+\zeta^2\rho_o^2\left(1-M_{\mathrm{N}}^2\right)}\ , \quad \mathcal{P}_e(\zeta) = \frac{M_{\mathrm{N}}^2\rho_o\sqrt{1-M_{\mathrm{N}}^2}}{\left[M_{\mathrm{N}}^2+\zeta^2\rho_o^2\left(1-M_{\mathrm{N}}^2\right)\right]^{3/2}}\ . \tag{31}$$

Here K is unity when the integrand functions equal unity. Splitting (30) into longitudinal and transverse kinetic-energy contributions with the definition $K = L + T$ for both two-dimensional and three-dimensional cases results at order $\epsilon\dot{q}|k|^{-1}$ in

$$L_{\mathrm{A}e} = 2\int_0^1 |B_{ue}|A_{ue}\left[1+\zeta^2\rho_o^2\left(M_{\mathrm{N}}^{-2}-1\right)\right]^{1/2}\mathcal{P}_e\mathrm{d}\zeta \tag{32a}$$

and

$$T_{\mathrm{A}e} = 2\int_0^1 |B_{ve}|A_{ve}\left[1+\zeta^2\rho_o^2\left(M_{\mathrm{N}}^{-2}-1\right)\right]^{1/2}\mathcal{P}_e\mathrm{d}\zeta\ . \tag{32b}$$

The amplitudes B_{ue} and B_{ve} are provided in (A11a), and the components A_{ue} and A_{ve} in given in (A12).

Since the normalization of the turbulent kinetic energy is different for upstream vorticity $K_{\mathrm{A}r}$ and upstream density $K_{\mathrm{A}e}$ disturbances, to facilitate comparisons use is made of the exothermic deviation factor $\Delta_{\mathrm{K}} = K_{\mathrm{A}}/K_{\mathrm{B}}$ defined previously, which holds for both $K_{\mathrm{A}r}$ and $K_{\mathrm{A}e}$, as does $\Delta_{\mathrm{L}} = L_{\mathrm{A}}/L_{\mathrm{B}}$ and $\Delta_{\mathrm{T}} = T_{\mathrm{A}}/T_{\mathrm{B}}$. It can be seen in Fig. 4 that the upstream entropic disturbances (gray curves) produce positive deviations for Δ_{L}, Δ_{T}, and Δ_{K}, while the upstream rotational fluctuations (black curves) generate negative deviations, except for the longitudinal Δ_{L} at high Mach numbers. Since the effect of the heat-release rate $\dot{q}$ is factored out, the results are universal and valid for any q. They are, however, meaningful only if $M_o \geq M_{cj}$, and since M_{cj} increases with q according to (3), the range of relevance decreases with increasing q. To provide an indication of the ranges, the curves are shown dashed in the figure for $M_o \lesssim 2.4$, which corresponds to $M_o = M_{cj}$ for $q = 1$. For strong overdrive, the effect of heat-release rate on the turbulent kinetic energy reaches a constant value. As a representative indication of the magnitudes of the effects, it may be observed that a detonation with $M_o = 3$ will modify the kinetic energy by $\pm\ 10\dot{q}|k|^{-1}$ %, negative if rotational and positive if entropic. As expected from the results for monochromatic disturbances, the heat release decreases the turbulent kinetic energy of rotational disturbances for both thick and thin detonations, while with purely entropic initial fluctuations, the heat release in the detonation decreases it for thin detonations but increases it for thick detonations

B. Downstream enstrophy

The effect of the inert shock front on the enstrophy levels is given in (A15) and agrees with previous results in shock-turbulence interactions[14,18]. The two-dimensional and three-dimensional contributions of order $\epsilon\dot{q}|k|^{-1}$ are, respectively,

$$W_{\mathrm{A}r} = \frac{1}{a_o^2}\int_0^1 \frac{|B_{\omega r}|A_{\omega r}\mathcal{P}_r}{\left[1+\zeta^2\rho_o^2\left(M_{\mathrm{N}}^{-2}-1\right)\right]^{1/2}}\mathrm{d}\zeta\ , \quad W_{\mathrm{A}r} = \frac{2}{3a_o^2}\int_0^1 \frac{|B_{\omega r}|A_{\omega r}\mathcal{P}_r}{\left[1+\zeta^2\rho_o^2\left(M_{\mathrm{N}}^{-2}-1\right)\right]^{1/2}}\mathrm{d}\zeta \tag{33}$$

for rotational disturbances. For entropic disturbances, there is generation of vorticity, and following the same reasoning as in (30), we normalize the enstrophy downstream as in[1,15], so the contribution for both two and three dimensions become

$$W_{\mathrm{A}e} = \int_0^1 \frac{2|B_{\omega e}|A_{\omega e}\mathcal{P}_e}{\left[1+\zeta^2\rho_o^2\left(M_{\mathrm{N}}^{-2}-1\right)\right]^{1/2}}\mathrm{d}\zeta\ . \tag{34}$$

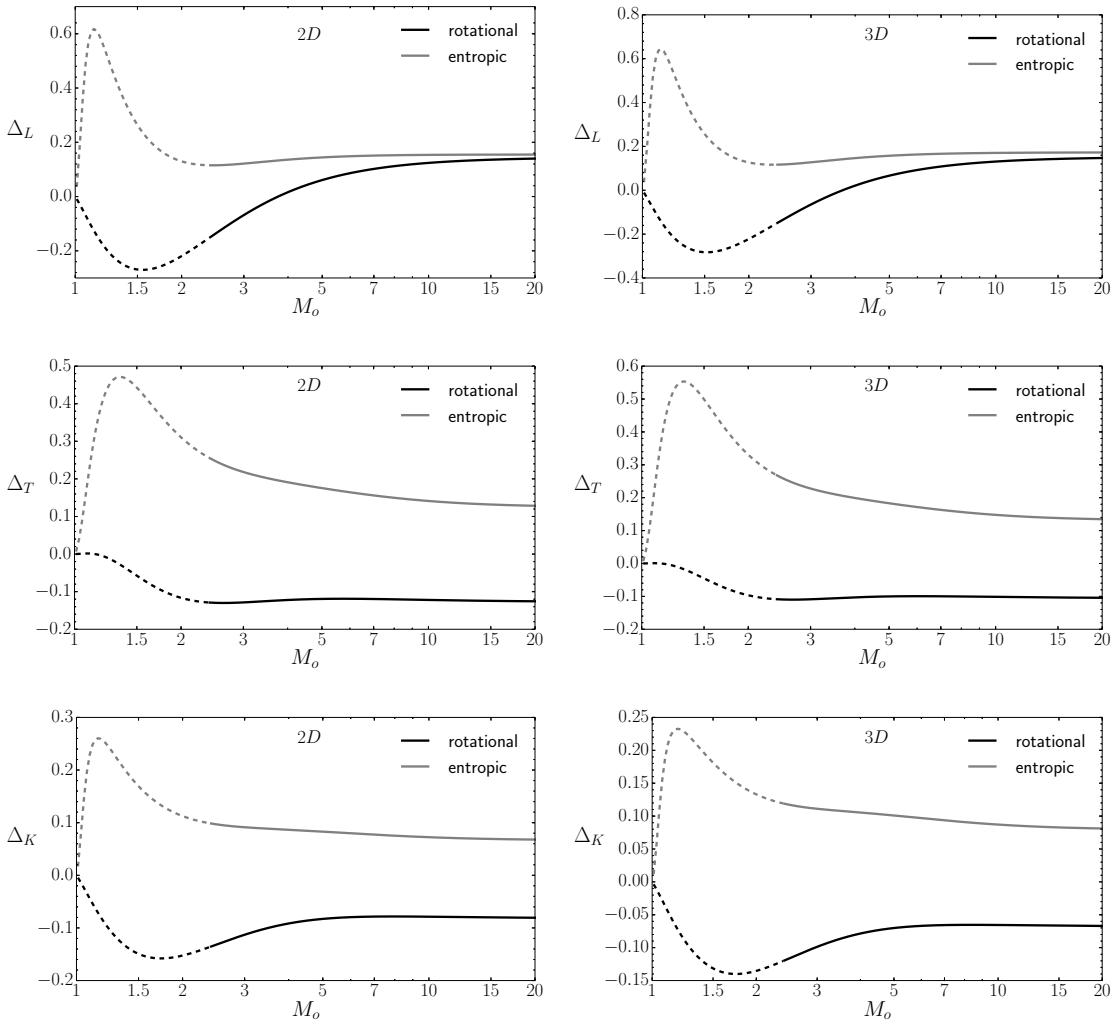

FIG. 4. Turbulent kinetic-energy deviations as functions of the shock Mach number M_o for two-dimensional (left panel) and three-dimensional (right panel) cases. The black and gray curves correspond to purely rotational ($\epsilon_e = 0$) and purely entropic ($\epsilon_r = 0$) disturbances upstream, respectively.

Figure 5 shows the enstrophy deviation $\Delta_{\rm W} = W_{\rm A}/W_{\rm B}$ for $\gamma = 1.2$ as a function of the shock strength M_o, in the same fashion as in Fig. 4. It is seen that $\Delta_{\rm W}$ grows unbounded for very weak shocks when there are no vorticity perturbations upstream. This occurs because, although both $W_{{\rm A}e}$ and its base contribution $W_{{\rm B}e}$ (see Fig.5 in Ref.[1]) approach zero when $M_o \cong 1$, the base contribution does so faster, but it is unimportant because weak-shock limits are not relevant to the Mach-number domains of common detonations. The general conclusions to be drawn from Fig. 5 are the same as those drawn from Fig. 4.

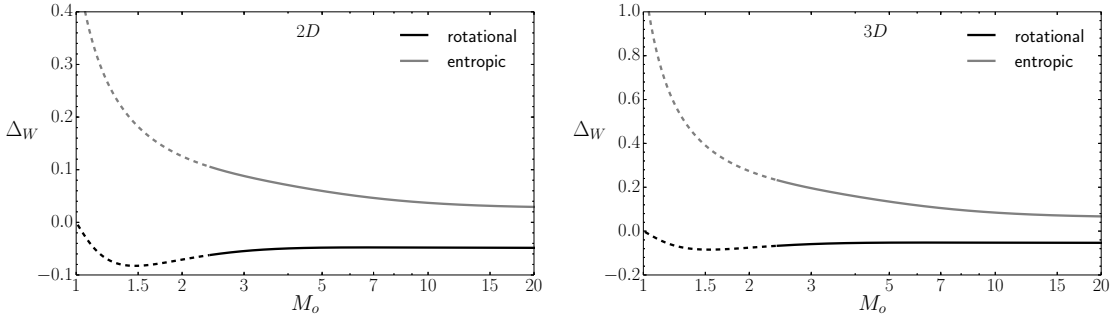

FIG. 5. Enstrophy deviation as a function of the shock Mach number M_o for two-dimensional (left panel) and three-dimensional (right panel) cases. The black and gray curves correspond to purely rotational ($\epsilon_e = 0$) and purely entropic ($\epsilon_r = 0$) disturbances upstream, respectively.

C. Downstream density

The average of the downstream square-density perturbations is denoted by $\langle \rho_b'^2 \rangle$, and for rotational upstream disturbances, following the same approach as for K, the factor G is defined as

$$G = \frac{2\langle \rho_b'^2 \rangle_{\rm 2D}}{\pi \int_0^\infty \epsilon_k(k)^2 k dk} = \int_0^\infty |\rho_b'|^2 \mathcal{P}_r \mathrm{d}\zeta \ , \quad G = \frac{3\langle \rho_b'^2 \rangle_{\rm 3D}}{8\pi \int_0^\infty \epsilon_k(k)^2 k^2 dk} = \int_0^\infty |\rho_b'|^2 \mathcal{P}_r \mathrm{d}\zeta \ , \quad (35)$$

for two-dimensional and three-dimensional cases, respectively, and the breakdown $G = G_{\rm B} + \dot{q}|k|^{-1} G_{\rm A}$ is introduced. The base contribution from rotational disturbances contains the entropic and acoustic fluctuations shown in (A17), and the contribution at order $\epsilon\dot{q}|k|^{-1}$ is

$$G_{{\rm A}r} = 2 \int_0^1 |B_{\rho r}| A_{\rho r} \left[1 + \zeta^2 \rho_o^2 \left(M_{\rm N}^{-2} - 1\right)\right]^{1/2} \mathcal{P}_r \mathrm{d}\zeta \quad (36)$$

for both two and three dimensions. For purely entropic fluctuations, the contribution at order $\epsilon q|k|^{-1}$ is

$$G_{{\rm A}e} = 2 \int_0^1 |B_{\rho e}| A_{\rho e} \ \mathcal{P}_e \mathrm{d}\zeta \ . \quad (37)$$

Figure 6 shows the associated average-density deviation factor $\Delta_{\rm G} = G_{\rm A}/G_{\rm B}$ as a function of the shock Mach number for $\gamma = 1.2$. It is observed that upstream entropic disturbances generate relative small contributions for the downstream density field at order $\dot{q}|k|^{-1}$, but the relative contribution of the upstream rotational disturbances is much greater because $G_{\rm B}$ is very small in that case. As in the previous Figs. 4 and 5, the factor $\Delta_{\rm G}$ is in qualitative agreement with the thin-detonation limit for rotational perturbations, but in the opposite direction for entropic perturbations.

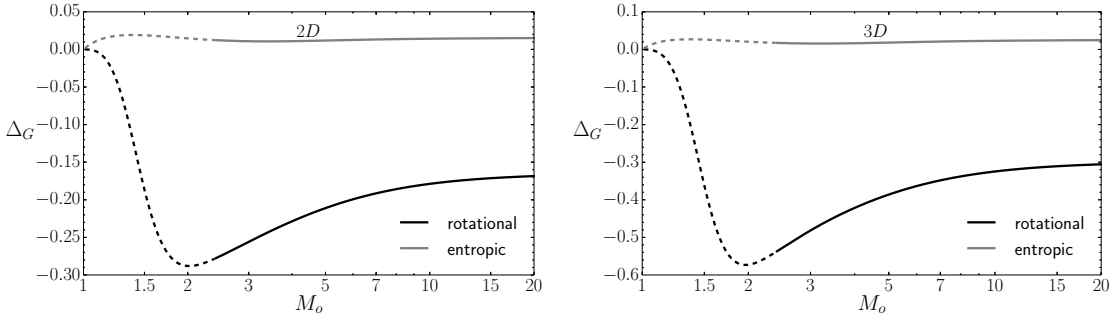

FIG. 6. Density deviation as a function of the shock Mach number M_o for two-dimensional (left panel) and three-dimensional (right panel) cases. The black and gray curves correspond to purely rotational ($\epsilon_e = 0$) and purely entropic ($\epsilon_r = 0$) disturbances upstream, respectively.

VII. CONCLUSIONS

To complement previous analyses of interactions of detonation with turbulence that treated all turbulence scales as being large compared with the thickness of the detonation, in the present work the turbulence scales were taken to be small compared with the thickness of the reaction zones that follow the lead inert shock in the detonation. Disturbances in the fresh mixture that involve only velocity fluctuations without any fluctuation of thermodynamic properties (rotational disturbances), and disturbances that involve fluctuations of the density of the fresh mixture without any velocity fluctuation (entropic disturbances) were considered separately, although results for cases in which both types of disturbances were present simultaneously are given in the appendix. It was found that, unlike the previous results for thin detonations, where the jump conditions across the complete detonation determined how the initial fluctuations were modified, for these thick detonations the modifications are affected mainly by the jump conditions across the leading inert shock. The wavelengths, frequencies, and phases of the disturbances vary as they pass through the heat-release zones, but the amplitudes do not, to leading order in the perturbations. Moreover, the effect of the rate of heat release $\dot{q}$ makes itself felt only right behind the lead shock, so that reaction-rate distributions are irrelevant, so long as they do not produce appreciable enthalpy changes over distances comparable with the disturbance wavelengths. Since real detonations often have endothermic pyrolysis regions behind the lead shock, before the heat release sets in, the fluctuations actually may respond as if the detonation were to absorb energy rather than releasing heat.

A finding that was not unexpected is that the influences on monochromatic fluctuations are strongest when the interaction occurs near the critical angle of incidence that separates downstream disturbances behind the lead shock that are supersonic from those that are subsonic. This motivated exhibiting results in a variable stretched about the critical angle, to maximize the efficiency of presentation. The expansion parameter of the analysis $\dot{q}|k|^{-1}$, essentially the product of the disturbance wavelength $|\bar{k}|^{-1}$ and the rate of heat release right behind the lead shock $\dot{\bar{q}}$, divided by the unperturbed enthalpy flux at the Neumann state $\bar{\rho}_{\mathrm{N}}\bar{u}_{\mathrm{N}}\bar{a}_{\mathrm{N}}^2/(\gamma-1)$, then factors out, and by normalizing quantities by their values at the Neumann state, parametric results can be presented with only the propagation Mach number M_o and the ratio of specific heats γ as parameters. A finding that was unexpected is that when the lead shock encounters the monochromatic fluctuations at an angle more head-on than the critical angle, and angle that results in generating propagating rather than evanescent acoustic perturbations, the influence of the heat-release rate on the disturbances is of second order in this small parameter. The leading-order results presented here, then, reflect only the influences of the interactions occurring at the larger angle θ, the encounters being more glancing than the critical angle. This is a peculiar result for thick detonations that does not have a counterpart for thin detonations.

For purely rotational disturbances (those without fluctuations of thermodynamic properties) in the fresh mixture, the heat release in the detonation reduces the relative fluctuation intensities downstream below the levels that would exist behind the inert lead shock, in both thin-detonation and thick-detonation limits. But for purely entropic disturbances in the fresh mixture (those without any velocity fluctuation), the effects of the heat release are the opposite in the two limits, the intensities being decreased for thin detonations but increased for thick detonations. This clearly suggests that when density fluctuations are dominant over velocity fluctuations, a situation thought to arise in turbulent flows at high Mach numbers[5], the influence of the passage of the detonation on the fluctuation field is affected qualitatively by the ratio of the detonation thickness to the range of sizes of the initial fluctuations. Smaller-scale fluctuations may be amplified, while longer-scale fluctuations are damped. The associated enhancement of smaller-scale disturbances may improve mixing rates and thereby promote combustion.

VIII. ACKNOWLEDGEMENTS

This work was supported by the U.S. AFOSR Grant No. FA9550-12-1-0138.

Appendix A: Appendix: More detailed and additional results

As indicated is Section 4, the base perturbations of order ϵ were obtained in previous work, namely in[14] for rotational fluctuations and in[15] for entropic fluctuations. The formulas are different for short-wavelength ($\zeta \geq 1$) and long-wavelength ($\zeta < 1$) cases, and only the latter appears in Section 4. In addition, the base pressure perturbations are affected by a second long-wavelength contribution that is orthogonal to the contribution in Section 4 and that therefore does not appear there. This second long-wavelength contribution will be identified by a prime, and the short-wavelength base perturbations will be identified by a double prime. Both of these influence later results, and therefore both are summarized here.

Addressing first the rotational contributions, it was found that[14]

$$B_{pr} = \frac{2M_oM_{\rm N}^2(1-\rho_o)\left[(M_o^2+1)\zeta^2-M_o^2\right]\left[M_{\rm N}^2-\rho_o\left(1-M_{\rm N}^2\right)\zeta^2\right]}{\rho_o^2\left(1-M_{\rm N}^2\right)\left[4M_o^4M_{\rm N}^2\zeta^2(\zeta^2-1)+\left((M_o^2+1)\zeta^2-M_o^2\right)^2\right]} \ , \tag{A1a}$$

$$B'_{pr} = -\frac{4M_o^3M_{\rm N}^3(1-\rho_o)\zeta\sqrt{1-\zeta^2}\left[M_{\rm N}^2-\rho_o\left(1-M_{\rm N}^2\right)\zeta^2\right]}{\rho_o^2\left(1-M_{\rm N}^2\right)\left[4M_o^4M_{\rm N}^2\zeta^2(\zeta^2-1)+\left((M_o^2+1)\zeta^2-M_o^2\right)^2\right]} \ , \tag{A1b}$$

and

$$B''_{pr} = \frac{2M_oM_{\rm N}^2(1-\rho_o)\left[M_{\rm N}^2-\rho_o\left(1-M_{\rm N}^2\right)\zeta^2\right]}{\rho_o^2\left(1-M_{\rm N}^2\right)\left[2M_o^2M_{\rm N}\zeta\sqrt{\zeta^2-1}+(M_o^2+1)\zeta^2-M_o^2\right]} \ . \tag{A1c}$$

The resulting amplitude of the asymptotic vorticity field generated by the upstream rotational mode is then

$$B_{\omega r} = \left[\left(\Omega_1+\Omega_2B_{pr}\right)^2+\left(\Omega_2B'_{pr}\right)^2\right]^{1/2} \ , \qquad B''_{\omega r} = \Omega_1+\Omega_2B''_{pr} \tag{A2}$$

where Ω_1 is the direct amplification contribution generated by compression effects, and Ω_2 is the associated shock-curvature effect, here given by

$$\Omega_1 = \frac{a_o\left[M_{\rm N}^2+\left(1-M_{\rm N}^2\right)\rho_o^2\zeta^2\right]}{\rho_oM_{\rm N}^2} \ , \qquad \Omega_2 = \frac{M_o^2\left(\gamma+1\right)\left(1-\rho_o\right)-2\left(M_o^2+1\right)}{4\rho_oM_o^2M_{\rm N}} \ . \tag{A3}$$

The associated density perturbations are

$$B_{\rho r} = \frac{1-M_o^2M_{\rm N}^2}{M_o^2M_{\rm N}^2}\left(B_{pr}^2+B_{pr}'^2\right)^{1/2} \ , \qquad B''_{\rho r} = \frac{1-M_o^2M_{\rm N}^2}{M_o^2M_{\rm N}^2}B''_{pr} \ . \tag{A4}$$

For the entropic contributions it was found that[15]

$$B_{pe} = -\frac{M_o^2 M_{\rm N}^2 (1-\rho_o)\left[(M_o^2+1)\zeta^2 - M_o^2\right]\left[M_{\rm N}^2 - \rho_o\left(1-M_{\rm N}^2\right)\zeta^2\right]}{\rho_o^2\left(1-M_{\rm N}^2\right)\left[4M_o^4 M_{\rm N}^2\zeta^2(\zeta^2-1) + \left((M_o^2+1)\zeta^2 - M_o^2\right)^2\right]} \ , \tag{A5a}$$

$$B'_{pe} = \frac{4M_o^4 M_{\rm N}^3 (1-\rho_o)\zeta\sqrt{1-\zeta^2}\left[M_{\rm N}^2 - \rho_o\left(1-M_{\rm N}^2\right)\zeta^2\right]}{\rho_o^2\left(1-M_{\rm N}^2\right)\left[4M_o^4 M_{\rm N}^2\zeta^2(\zeta^2-1) + \left((M_o^2+1)\zeta^2 - M_o^2\right)^2\right]} \ , \tag{A5b}$$

$$B''_{pe} = -\frac{M_o^2 M_{\rm N}^2 (1-\rho_o)\left[M_{\rm N}^2 - \rho_o\left(1-M_{\rm N}^2\right)\zeta^2\right]}{\rho_o^2\left(1-M_{\rm N}^2\right)\left[2M_o^2 M_{\rm N}\zeta\sqrt{\zeta^2-1} + (M_o^2+1)\zeta^2 - M_o^2\right]} \ . \tag{A5c}$$

The resulting the vorticity-disturbance coefficients are

$$B_{\omega e} = \left[\left(\Omega_3 + \Omega_2 B_{pe}\right)^2 + \left(\Omega_2 B'_{pe}\right)^2\right]^{1/2} \ , \quad B''_{\omega e} = \Omega_3 + \Omega_2 B''_{pe} \tag{A6}$$

where Ω_3 is the baroclinic contribution (i.e., it accounts for the vorticity caused by the streamwise pressure jump across the shock and transverse density fluctuations) and is given by

$$\Omega_3 = -\frac{M_{\rm N}\left(1-\rho_o^2\right)}{2\rho_o^2} \ . \tag{A7}$$

The corresponding amplitudes of the steady density perturbations are

$$B_{\rho e} = \left[\left(\frac{1-M_o^2 M_{\rm N}^2}{M_o^2 M_{\rm N}^2} B_{pe} + 1\right)^2 + \left(\frac{1-M_o^2 M_{\rm N}^2}{M_o^2 M_{\rm N}^2} B'_{pe}\right)^2\right]^{1/2} \ , \quad B''_{\rho e} = \frac{1-M_o^2 M_{\rm N}^2}{M_o^2 M_{\rm N}^2} B''_{pe} + 1 \ . \tag{A8}$$

Besides velocity fluctuations associated with the vorticity fluctuations addressed here, there are also acoustic contributions to the velocity perturbations, which will be identified with the superscript a. For rotational disturbances, the associated amplitudes of the x and y components are

$$B_{ur} = \frac{M_{\rm N}^2}{M_{\rm N}^2 + \left(1-M_{\rm N}^2\right)\zeta^2} B_{\omega r} \ , \qquad B_{vr} = \frac{\zeta M_{\rm N}\sqrt{1-M_{\rm N}^2}}{M_{\rm N}^2 + \left(1-M_{\rm N}^2\right)\zeta^2} B_{\omega r} \ , \tag{A9a}$$

while the acoustic contributions are

$$B^a_{ur} = \frac{k_a}{\omega_a \rho_b} B''_{pr} \ , \qquad B^a_{vr} = \frac{k_y}{\omega_a \rho_b} B''_{pr} \ . \tag{A9b}$$

The relationships in (A9a), written there for the long-wavelength cases, also apply for the short-wavelength cases. The corresponding contributions to the velocity field at order $\epsilon \dot{q} k_y^{-1}$ are

$$A_{ur} = \frac{M_{\rm N}^2}{M_{\rm N}^2 + \left(1-M_{\rm N}^2\right)\zeta^2} A_{\omega r} \ , \qquad A_{vr} = \frac{\zeta M_{\rm N}\sqrt{1-M_{\rm N}^2}}{M_{\rm N}^2 + \left(1-M_{\rm N}^2\right)\zeta^2} A_{\omega r} \ , \tag{A10}$$

where the factor $A_{\omega r}$ is defined in (21). For entropic disturbances the amplitudes are

$$B_{ue} = \frac{M_{\rm N}^2}{M_{\rm N}^2 + (1 - M_{\rm N}^2)\,\zeta^2} B_{\omega e} \ , \qquad B_{ve} = \frac{\zeta M_{\rm N}\sqrt{1 - M_{\rm N}^2}}{M_{\rm N}^2 + (1 - M_{\rm N}^2)\,\zeta^2} B_{\omega e} \ , \tag{A11a}$$

and

$$B_{ue}^a = \frac{k_a}{\omega_a \rho_b} B_{pe}'' \ , \qquad B_{ve}^a = \frac{k_y}{\omega_a \rho_b} B_{pe}'' \ , \tag{A11b}$$

for the rotational and acoustic contributions, respectively. Similarly, the vortical contributions to the velocity field at order at order $\epsilon \dot{q} k_y^{-1}$ are found to be

$$A_{ue} = \frac{M_{\rm N}^2}{M_{\rm N}^2 + (1 - M_{\rm N}^2)\,\zeta^2} A_{\omega e} \ , \qquad A_{ve} = \frac{\zeta M_{\rm N}\sqrt{1 - M_{\rm N}^2}}{M_{\rm N}^2 + (1 - M_{\rm N}^2)\,\zeta^2} A_{\omega e} \ , \tag{A12}$$

where the factors $A_{\omega e}$ are also provided in (21).

The longitudinal $L_{\rm B}$ kinetic energy generated by the inert shock when traveling through an isotropic rotational field is

$$L_{{\rm B}r} = \frac{1}{a_o^2}\int_0^1 (B_{ur})^2 \mathcal{P}_r {\rm d}\zeta + \frac{1}{a_o^2}\int_1^\infty (B_{ur}'')^2 \ \mathcal{P}_r {\rm d}\zeta + \frac{1}{a_o^2}\int_{\zeta^*}^\infty (B_{ur}^a)^2 \ \mathcal{P}_r {\rm d}\zeta \ , \tag{A13}$$

and the transverse $T_{\rm B}$ contributions to kinetic energy in two and three dimensions are, respectively

$$T_{{\rm B}r} = \frac{1}{a_o^2}\int_0^1 (B_{vr})^2 \ \mathcal{P}_r {\rm d}\zeta + \frac{1}{a_o^2}\int_1^\infty (B_{vr}'')^2 \ \mathcal{P}_r {\rm d}\zeta + \frac{1}{a_o^2}\int_{\zeta^*}^\infty (B_{vr}^a)^2 \ \mathcal{P}_r {\rm d}\zeta \tag{A14a}$$

and

$$T_{{\rm B}r} = \frac{1}{2a_o^2}\int_0^1 (B_{vr})^2 \ \mathcal{P}_r {\rm d}\zeta + \frac{1}{2a_o^2}\int_1^\infty (B_{vr}'')^2 \ \mathcal{P}_r {\rm d}\zeta + \frac{1}{2a_o^2}\int_{\zeta^*}^\infty (B_{vr}^a)^2 \ \mathcal{P}_r {\rm d}\zeta + \frac{3}{4} \ . \tag{A14b}$$

When the upstream flow consists of isotropic solenoidal perturbations, the amplification of those perturbations in two and three dimensions is, respectively,

$$W_{{\rm B}r} = \frac{1}{2a_o^2}\int_0^1 \frac{(B_{\omega r})^2 M_{\rm N}^2 \ \mathcal{P}_r}{M_{\rm N}^2 + \zeta^2 \rho_o^2 \,(1 - M_{\rm N}^2)} {\rm d}\zeta + \frac{1}{2a_o^2}\int_1^\infty \frac{(B_{\omega r}'')^2 M_{\rm N}^2 \ \mathcal{P}_r}{M_{\rm N}^2 + \zeta^2 \rho_o^2 \,(1 - M_{\rm N}^2)} {\rm d}\zeta \ , \tag{A15a}$$

and

$$W_{{\rm B}r} = \frac{1}{3} + \frac{1}{6\rho_o^2} + \frac{1}{3a_o^2}\int_0^1 \frac{(B_{\omega r})^2 M_{\rm N}^2 \ \mathcal{P}_r}{M_{\rm N}^2 + \zeta^2 \rho_o^2 \,(1 - M_{\rm N}^2)} {\rm d}\zeta + \frac{1}{3a_o^2}\int_1^\infty \frac{(B_{\omega r}'')^2 M_{\rm N}^2 \ \mathcal{P}_r}{M_{\rm N}^2 + \zeta^2 \rho_o^2 \,(1 - M_{\rm N}^2)} {\rm d}\zeta \ , \tag{A15b}$$

where the three-dimensional contribution can be split into $W_{\mathrm{B}r} = 1/3 + 2/3W_\perp$, $W_\perp$ being the transverse contribution, $W_\perp = 1/4\rho_o^{-2} + 3/4W_z$. The behavior of the transverse vorticity $W_\perp$ can be found in Fig. 4 of Ref.[18] and Fig. 26 of Ref.[14]. If there is no vorticity perturbations upstream, the enstrophy downstream is redefined as[15]

$$W_{\mathrm{B}e} = \int_0^1 \frac{(B_{\omega e})^2 M_{\mathrm{N}}^2 \mathcal{P}_e}{M_{\mathrm{N}}^2 + \zeta^2 \rho_o^2 (1 - M_{\mathrm{N}}^2)} \mathrm{d}\zeta + \int_1^\infty \frac{(B''_{\omega e})^2 M_{\mathrm{N}}^2 \mathcal{P}_e}{M_{\mathrm{N}}^2 + \zeta^2 \rho_o^2 (1 - M_{\mathrm{N}}^2)} \mathrm{d}\zeta \ , \tag{A16}$$

and detailed study of the enstrophy generated by shock-entropy interaction may be found in Refs.[15,20]. The inert base contribution to the square-density perturbations behind the detonation, defined by (35), is[1]

$$G_{\mathrm{B}r} = \int_0^1 (B_{\rho r})^2 \mathcal{P} \mathrm{d}\zeta + \int_1^\infty (B''_{\rho r})^2 \mathcal{P}(\zeta) \mathrm{d}\zeta + \frac{1}{a_b^4} \int_1^\infty (B^a_{pr})^2 \mathcal{P} \mathrm{d}\zeta \ , \tag{A17}$$

where $\mathcal{P}$ stands for $\mathcal{P}_e$ or $\mathcal{P}_r$ depending on whether rotational or entropic perturbations are considered.

When there are both rotational and entropic fluctuations upstream, phase shifts introduce interferences that prevent results from being obtained by simply adding the separate contributions. Previous work[21,22] has addressed the two cases $\epsilon_e = \epsilon_r M_o^{-1}$ and $\epsilon_e = -\epsilon_r M_o^{-1}$ with the same spectral density distribution for each type of fluctuations. Corresponding results from the present formulation are shown in Fig. 7, where it is seen that, for the moderate-to-strong shocks of interest, all of the deviation factors are negative, irrespective of the sign of the correlation. This may be expected from Figs. 4-6, in view of the domination of the rotational fluctuations at high M_o for the selected combination of ϵ_r and ϵ_e. The negative correlation does show a positive peak at lower M_o, but this is unlikely to lie in the range of realistic detonations. If ϵ_e had been chosen to be proportional to $\epsilon_r M_o$ instead of $\epsilon_r M_o^{-1}$, as it would be for the disturbances suggested by Morkovin[5], then the entropic contribution would be much more important at high Mach numbers. The choice made for Fig. 7 was to facilitate comparison with corresponding results in the literature[21,22].

REFERENCES

[1]C. Huete, A.L. Sánchez, and F.A. Williams. Theory of interactions of thin strong detonations with turbulent gases. *Physics of Fluids*, 25:076105, 2013.

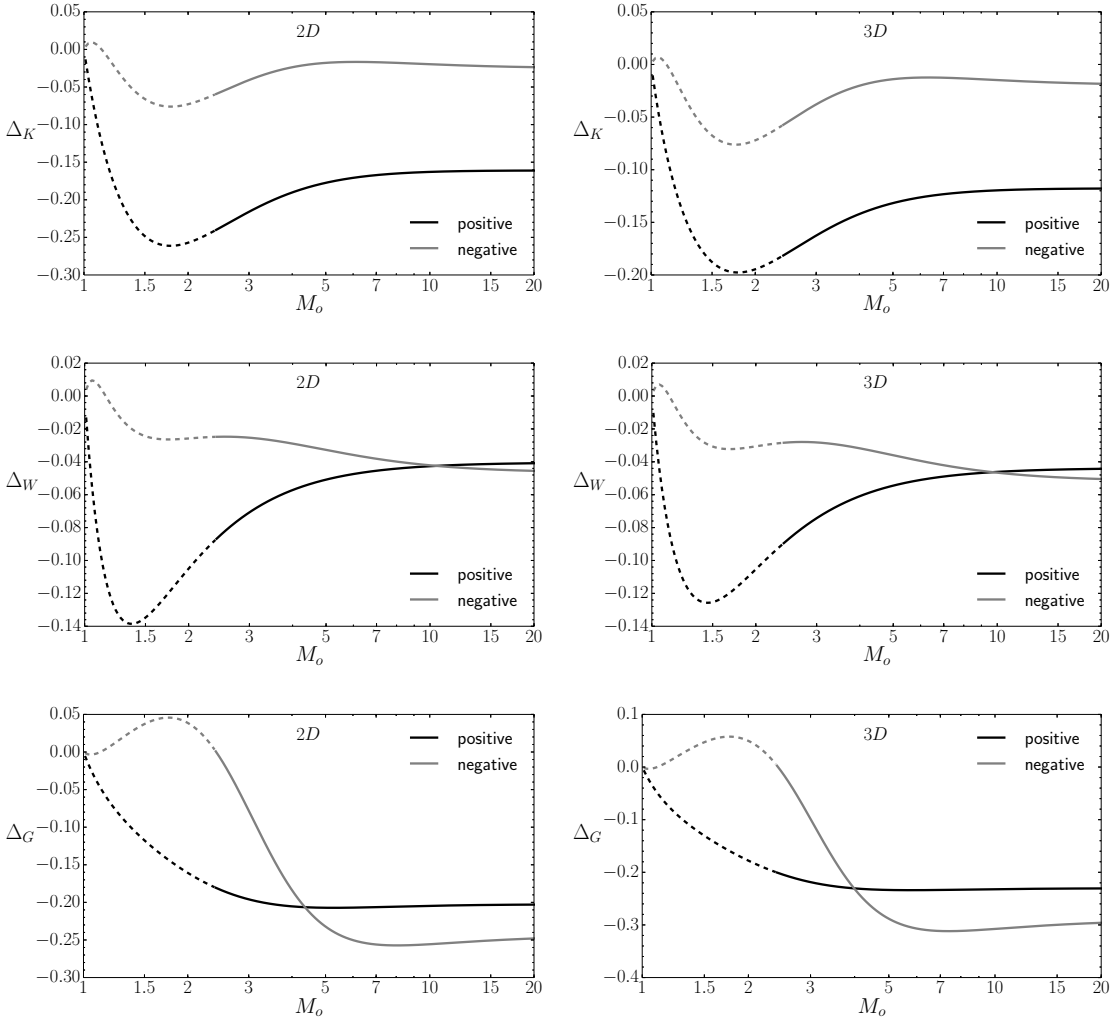

FIG. 7. Turbulent kinetic-energy, enstrophy and density deviations as functions of the shock Mach number M_o for two-dimensional (left panel) and three-dimensional (right panel) cases. The black and gray curves correspond to purely rotational ($\epsilon_e = 0$) and purely entropic ($\epsilon_r = 0$) disturbances upstream, respectively.

[2]T.L. Jackson, A.K. Kapila, and M.Y. Hussaini. Convection of a pattern of vorticity through a reacting shock wave. *Physics of Fluids A: Fluid Dynamics*, 2:1260, 1990.

[3]T.L. Jackson, M.Y. Hussaini, and H.S. Ribner. Interaction of turbulence with a detonation wave. *Physics of Fluids A: Fluid Dynamics*, 5(3):745–749, 1993.

[4]B.T. Chu and L.S.G. Kovásznay. Non-linear interactions in a viscous heat-conducting compressible gas. *Journal of Fluid Mechanics*, 3(05):494–514, 1958.

[5]M. V. Morkovin. Effects of compressibility on turbulent flows. *In Mechanique de la Turbulence, A. Favre (Ed.), CNRS, Paris*, pages 367–380, 1962.

[6]K. Kailasanath. Review of propulsion applications of detonation waves. *AIAA journal*, 38(9):1698–1708, 2000.

[7]G. Fusina. *Numerical investigation of oblique detonation waves for a shcramjet combustor*. PhD thesis, 2003.

[8]L. Massa, M. Chauhan, and F.K. Lu. Detonation-turbulence interaction. *Combustion and Flame*, 158:1788–1806, 2011.

[9]L. Massa and F.K. Lu. The role of the induction zone on the detonationation-turbulencelinear interaction. *Combustion Theory and Modelling*, 15(3):347–371, 2011.

[10]Y.B Zel'dovich. On he theory of the propagation of detonations in gaseous systems. *Zhur. Eksp. Teor. Fiz.*, 10:542.568, 1940.

[11]J. von Neumann. Theory of detonation waves. *Prog. Rept. No. 238, (Report 549, O.S.R.D, National Defense Research Committee Div. B*, 1942.

[12]W. Doring. On the detonation process in gases. *Ann. Physik*, 43:421–436, 1943.

[13]H. S. Ribner. Convection of a pattern of vorticity through a shock wave. *NACA Report*, 1164, 1954.

[14]J.G. Wouchuk, C. Huete Ruiz de Lira, and A.L. Velikovich. Analytical linear theory for the interaction of a planar shock wave with an isotropic turbulent vorticity field. *Phys. Rev. E*, 79(6):066315, 2009.

[15]C. Huete Ruiz de Lira, A.L. Velikovich, and J.G. Wouchuk. Analytical linear theory for the interaction of a planar shock wave with a two- or three-dimensional random isotropic density field. *Phys. Rev. E*, 83(5):056320, 2011.

[16]G.K. Batchelor. *The theory of homogeneous turbulence*. Cambridge university press, 1953.

[17]H. S. Ribner. Shock-turbulence interaction and the generation of noise. *NACA Report*, 1233, 1955.

[18]S Lee, S. K. Lele, and P. Moin. Interaction of isotropic turbulence with shock waves: effect of shock strength. *Journal of Fluid Mechanics*, 340:225–247, 1997.

[19]C. Huete, J.G. Wouchuk, B. Canaud, and A.L. Velikovich. Analytical linear theory for the shock and re-shock of isotropic density inhomogeneities. *Journal of Fluid Mechanics*, 700:214–245, 2012.

[20]BM Johnson and O Schilling. Reynolds-averaged navier–stokes model predictions of linear instability. i: Buoyancy-and shear-driven flows. *Journal of Turbulence*, (12), 2011.

[21]K. Mahesh, S. K. Lele, and P. Moin. The influence of entropy fluctuations on the interaction of turbulence with a shock wave. *Journal of Fluid Mechanics*, 334:353–379, 1997.

[22]V. K. Veera and K. Sinha. Modeling the effect of upstream temperature fluctuations on shock/homogeneous turbulence interaction. *Physics of fluids*, 21:025101, 2009.